Optimization strategy for encapsulation efficiency and size of drug loaded silica xerogel/polymer core-shell composite nanoparticles prepared by gelation-emulsion method

W.F. Huang[1], Gary C.P. Tsui*[1], C.Y. Tang[1], M. Yang[2]

[1]Department of Industrial and Systems Engineering, The Hong Kong Polytechnic University, Hung Hom, Kowloon, Hong Kong, China

[2]Interdisciplinary Division of Biomedical Engineering, The Hong Kong Polytechnic University, Hung Hom, Kowloon, Hong Kong, China

*Corresponding author: E-mail address: mfgary@polyu.edu.hk

ABSTRACT

It has been commonly discovered that reducing particle size always accompanies with undesirable deterioration of drug encapsulation efficiency in double emulsion based techniques. However, a clear optimization strategy for process variables to minimize this negative impact has been rarely reported. To fill this gap, we have successfully developed an optimization strategy for silica xerogel/polymer composite nanoparticles prepared by our recently developed gelation-emulsion method. To develop this strategy, interactive effects of multiple process variables were investigated through a 4-factor 3-level experimental design by considering all screened dominant process variables influencing particle size and encapsulation efficiency, including sonication time of second emulsion (t_2), sonication power of the second emulsion (P_2), total volume of the second emulsion (V_2) and volume ratio of aqueous phase and primary emulsion (r). The optimization strategy for fabricating the target particle size with optimal encapsulation efficiency was designed by adjusting the process variables in the order of r, V_2, t_2 and P_2 With this strategy, conspicuous enhancement of the encapsulation efficiency (e.g. from 27 to 63% for a particle size of 211 nm) and significant increment of the feasible size range through our novel fabrication method from 192~569 nm to 90~914 nm have been achieved in this study.

Keywords: Optimization strategy, Encapsulation, Experimental design, Double emulsion, Composite nanoparticles, Drug delivery

INTRODUCTION

Polymer nanoparticles have been attractive vehicles for high efficient drug delivery, owing to their enhanced permeability and retention (EPR) effects that can deliver active molecules to target disease sites, which significantly improve the therapeutic efficiency and reduce side-effects [1-3]. Various techniques, such as double emulsion, single emulsion, emulsions-diffusion, nanoprecipitation and salting out processes, have been developed to prepare theses nanoparticles [4-6]. Among all these techniques, double emulsion process possesses a unique advantage of being capable to encapsulate both hydrophilic and hydrophobic drugs; while other techniques are mostly limited to the encapsulations of hydrophobic drugs. This unique characteristic of double emulsion makes it a popular and promising process for encapsulation of water soluble active ingredients. However, it has been discovered in most investigations that reduction of particle size always accompanies with undesirable deterioration of drug encapsulation in double emulsion based techniques [7-12]. To mitigate this common problem, it is necessary to develop an optimization strategy to explore optimal combinations of all the significant process parameters that can minimize the reduction of encapsulation efficiency (EE) for decreasing the particle size.

Effects of process variables are usually investigated through single variable studies as reported in most publications [13, 14]. However, it is difficult to devise a clear optimization strategy from these single variable studies. For instance, it can be concluded from a single variable study that increasing the emulsification time led to

smaller particle size and unwanted reduced EE, while the values of other variables were kept constant. However, this single variable study could not indicate how the tendency would change or whether deterioration of EE could be avoided, when the values of other variables were changed simultaneously. To answer these questions, studies of these interactive effects are needed. Interactive effects among variables are usually investigated through formal experimental designs. Compared with the single variable study, relatively few research studies focused on the interactive effects of multiple variables. According to Feczkó et al[15, 16], the effects of various fabrication parameters of polymer concentration, concentration of polyvinyl alcohol (PVA, emulsifier), concentration of active ingredient, volume ratio of external aqueous phase (W_2 phase) and primary emulsion, emulsification time of the second emulsion time on size and encapsulation efficiency of PLGA nanoparticles were analyzed by a 5-factorial 3-level Box–Behnken experimental design. However, the effects of many significant process variables, such as sonication power output (emulsification power) and the volume ratio of W_2 phase were not included in their study, and thus a clear optimization strategy to find proper combinations of variables on the target size and optimal EE could not be provided. This may result from the fact that both compositional and process variables were considered, making it difficult to obtain a clear optimization strategy. In view of this, first determination of significant process variables and thus development of an optimization strategy are required.

Biodegradable polymers, such as Poly (L-lactide) and Poly (lactic-co-glycolic acid), are widely adopted to fabricate nanoparticles because of their controllable degradability and biocompatibility [17-21]. However, applications of these biodegradable polymers are limited by their weak mechanical strength and the inflammatory tissue responses that are caused by inherently acidic, pro-inflammatory degradation products [22]. Compared with these polymers, sol-gel processed silica xerogels have the intrinsic advantages of higher chemical, thermal and electrical stability, better mechanical properties and a favorable tissue response [23-25]. These silica xerogels are amorphous and bioresorbable, and have a highly porous silica (SiO_2) form prepared by the sol-gel technology under mild process conditions [26-28]. Drug release from silica xerogel has been found to be related to its physical properties, such as porosity, density and internal structure, which can be easily adjusted by manipulating the parameters of the sol-gel chemistry[29, 30]. However, severe burst release was discovered using the silica xerogel alone as drug carriers because of its high porosity[31]. To overcome the shortages of both silica xerogel and biopolymer as drug carriers, drug loaded silica xerogel core-polymer shell composite nanoparticles for drug delivery have been fabricated in our previous work by developing a novel gelation-emulsion method with integration of both double emulsion and sol-gel techniques[12]. The negative impacts of reducing the particle size on EE were also observed during development of this novel method. In view of this, an optimization strategy is necessary for mitigating the negative impacts of decreasing particle size on EE.

With the introduction of silica xerogel, the prepared composite nanoparticles in our previous study, as compared with the polymeric nanoparticles, have been proved to possess a higher encapsulation efficiency (71.8% vs 34.2%), lower burst drug release (50% vs 80%) for better controlled drug release applications, and much longer drug complete release time (66 days vs 20 days) suitable for long-term sustained drug delivery applications[12]. Size and EE of the composite nanoparticles can be well controlled in the range of 192~569 nm with a maximum encapsulation efficiency of 82% through adjusting the values of sonication time and concentration of emulsifier (PVA)[12]. The size range of the nanoparticles achieved by our recently developed gelation-emulsion method is 192~569 nm. However, only some of the major effects were considered through the single variable study in our previous study, limiting the operation window of the gelation-emulsion method (e.g. feasible size range). In order to broaden this operation window, it would be worthy of developing of an optimization strategy by considering the interactive effects among all the significant process variables.

The aim of this study was to develop an optimization strategy to explore the optimal combinations of the process variables based on gelation-emulsion technique for tailored size and optimal encapsulation efficiency of drug loaded xerogel/silica nanoparticles through a factorial experimental design. This study contributes to mitigating the negative impacts of decreasing particle size on EE. To develop such a strategy, all the significant process variables and corresponding influences on the particle size and EE

were firstly determined through theoretical analysis. Interactive effects of multiple variables were then investigated by a 4-factor 3 level central composite face-centered experimental design (CCF). Empirical models for correlating the size and EE of the nanoparticles with the process variables were established to confirm and quantify the influences of the selected process variables. The developed optimization strategy can also be applied to the other double emulsion based techniques for fabrication of nanoparticles for drug delivery.

EXPERIMENTAL

To develop the optimization strategy, the dominant process variables were firstly determined through analysis of current investigation. The influences of the selected process variables on the particle size and EE were estimated by studying the principles of formation of emulsion. To confirm these estimations, a 4-factor 3-level factorial design was performed before conducting the experiments. Afterward, materials, fabrication procedures and characterizations of the nanoparticles are described.

Determination of dominant process variables

The impacts of various fabrication parameters of double emulsion based techniques on the size and EE have been extensively investigated. According to the study of Azizi et al [8], drug concentration, emulsifier characteristics and sonication power output were found to have significant impacts on the size and EE of nanoparticles. Increasing the

polymer concentration was found to result in larger EE and particle size; while increasing the emulsification time led to the reduction of the size and EE of nanoparticles [9]. A screening design methodology was adopted by Al Haushey et al [32] to evaluate the effects of over 12 process and formulation variables on the size and EE of nanoparticles prepared by the double emulsion method. It can be summarized from their studies and other investigations that the size and EE of nanoparticles are significantly related to the concentration of polymer/active substance/emulsifier, emulsification time/power, volume of W_2 phase and volume ratio of W_2 and primary emulsion [7-11, 32-34]. All the variables in double emulsion can be categorized as process variables (e.g. emulsification time/power, volume of W_2 phase, and volume ratio of W_2 phase and primary emulsion et al.) and formulation variables (e.g. polymer type, polymer/active substance/emulsifier concentration). The influences of the process variables were focused in the present study. From the analysis above, the dominant process variables were determined to be sonication time of the second emulsion, t, sonication power of the second emulsion, p_t, total volume of the second emulsion, v and volume ratio of W_2 phase and primary emulsion, r.

Influences of the dominant variables on size and EE

In order to gain an insight into the influences of these process variables, it is necessary to start with understandings of the formations of emulsion under ultrasonic emulsification process and subsequently analyze the effect of each variable.

Generally, an oil phase (dispersed phase), an aqueous phase (continuous phase) and emulsifiers (such as surfactants) are required. *O/W* emulsion is actually an aqueous suspension of tiny oil droplets in the presence of the emulsifier. In order to disperse the oil phase into the aqueous phase, a certain amount of energy is required to expand and disintegrate the bulk dispersed phase into large number of tiny droplets. This high energy can also be understood from an aspect of the Laplace pressure, p that is defined as a pressure gap between inner and outside pressure of spherical droplets due to existence of interfacial tension [35]:

$$p = \frac{2\sigma}{R} \tag{1}$$

where R is the principal radii of the curvature of the droplets and σ is the surface tension.

In order to deform and then break up large droplets into smaller ones, certain energies are required to provide external stress or effective surfactants are needed to reduce the interfacial surface tension. However, the effect of the surfactant and the interfacial surface tension, σ in the current discussion was considered to be a constant, because the surfactant and its concentration are the same in every trial. It can be concluded from equation (1) that higher energies are required to generate small droplets (such as nano-droplets) rather than large droplets (micro-droplets).

The high energies are usually supplied by various homogenizers, such as micro-fluidizer, high pressure homogenizer and ultrasound homogenizer. In current case, the ultrasound homogenizer is selected, because of its uniform emulsification effect, cost-effectiveness and user-friendliness. There are primarily two mechanisms to explain the formation of emulsion under the influence of ultrasound: capillary waves and cavitation [36, 37]. For a practical condition, the cavitation is generally regarded as the primary effect. In this case, cavitation bubbles are generated in a sonicated medium in a sonication environment. The ultrasound waves in the liquid media generate a series of periodic cycles of compression and rarefaction. During rarefaction, cavitation bubbles are created when the negative pressure outweighs the attractive forces between liquid molecules. Filled with the vapor or gas generated on the interface, these cavitation bubbles do not collapse during the compression cycles. Instead, they continue to grow until reaching an unstable critical size and then collapse. These violent collapses lead to the formation of intensive shear fields and microjets of high velocity liquid in the vicinity of collapsing bubbles, which cause formation of turbulent micro-streams, and are also known as the source of energy for emulsification.

The formation of emulsion is the process the break-up of large bulk dispersed phase or large droplets of dispersed phase. Analysis of the droplet break-up can be divided into two patterns: break-up in a laminar flow and break-up in a turbulent flow [38]. The droplet break-up in the laminar flow is not suitable for the continuous phase of low viscosity. Considering the facts that low viscous continuous phases are used in current

study and turbulent micro-stream is generated under ultrasound, the pattern of the droplet break-up in the turbulent flow is more appropriate for the analysis of the ultrasound emulsion.

During the turbulent flow, a spectrum of eddies with various sizes is generated. These eddies contribute to pressure fluctuations. According to the Kolmogorov theory, if the pressure exceeds the Laplace pressure p (equation (1)) of an adjoining droplet of diameter X, the droplet would be broken up [38]. This leads to formation of the largest droplets that can remain in the turbulent flow regime. The maximum droplet diameter is given by an empirical equation [39]:

$$d_{max} = X_{max} = C P_v^{-0.4} \sigma^{0.6} \rho^{-0.2} \quad (2)$$

where C is a constant and ρ is the density of continuous phase. Because of the heterogeneous turbulent field, the resulting droplet would exhibit a spread in the size or a size distribution with an average diameter, d_{av}. This empirical equation was developed by considering an emulsion that was composed of oil, water and surfactants and was generated with the energy inputs similar with the emulsion prepared in the current study. However, considering the fact that the compositions of these phases and surfactants were different, it was merely assumed that this equation was applied to qualitative determination of the influences of process variables in current case. This assumption was further tested by experimental results as discussed in the following section.

Equation (2) can also be applied to d_{av} by varying the value of constant C,

$$d_{av} = BP_v^{-0.4}\sigma^{0.6}\rho^{-0.2} \quad (3)$$

where B is also a constant but different from C. The power density, P_v (W/mL), the average energy dissipated per unit time and unit volume, is the primary parameter characterizing the turbulent.

Through a dimensional analysis, the power density P_v can be expressed as:

$$P_v = \frac{P_t}{V} \quad (4)$$

where P_t is the sonication power output of the ultrasonic homogenizer and V is the volume of the emulsion. It can be noted from equations (3) and (4) that the average size of the droplets, which directly governs the average size of composite nanoparticles, is proportional to the sonication power output, P_t and inversely proportional to the total volume of the emulsion, V.

As the sonication power output, P_t is defined as the work or energy, E divided by working time, t, equation (*4*) is written as

$$P_v = D\frac{E}{Vt} \quad (5)$$

Since the energy conversion of sonication power was not 100% in the present work due to the limitation of the sonication device, a constant D was added to calibrate this energy conversion gap. The total volume of emulsion, V is comprised of the dispersed phase volume, V_d and the continuous phase volume, V_c. Volume ratio (r) is defined in terms of the continuous phase and the dispersed phase as

$$r = \frac{V_c}{V_d} \tag{6}$$

Equation (6) can then be substituted to

$$P_v = \frac{E}{V_d(1+r)t} \tag{7}$$

where r is independent of V_d. It can be observed from equations (6) and (7) that the working time, t and the volume ratio, r are inversely proportional to the average diameter of the dispersed phase droplets and thus the particle size of the composite nanoparticles.

For the present study, the dispersed phase was the primary emulsion (W_1/O), while the continuous phase (W_2) was fixed to be 1.5 w% PVA aqueous solutions. The emulsion process was described as droplet break-up in the turbulent flow. Hence, the process variables of emulsification influenced not only the particle size but also the encapsulation efficiency of the nanoparticles. Estimations of the influences of these parameters on the particle size and EE are summarized in Table 1. The following factorial experimental design aimed to verify the assumptions and quantify the effects of each process variable on the size and encapsulation efficiency of the prepared composite nanoparticles.

Experimental Design and Analysis

All selected process variables and corresponding study intervals are summarized in Table 2. A 4-factor 3 level central composite face-centered experimental design (CCF)

with two center points is chosen for vastly reducing experimental works without remarkably losing essential information. The design was divided into two parts: linear analysis and non-linear analysis. The unique advantage of applying CCF is that a designer can determine the experimental necessity for non-linear analysis based on the results of linear analysis. For instance, if the linear influence evaluation indicates a strong linear behavior and weak curve behavior, further experiments for non-linear analysis would be unnecessary. By utilizing the CCF method, a total of 27 experiments with different combination of process variables were designed as shown in Table 3.

Design and analysis of experiment are carried out using SAS JMP software package. Combinations of process variables and the corresponding responses are shown in Tables 2 and 3. Linear and quadratic effects and their linear-linear interactions of all selected process variables with dependences on the size and EE were firstly analyzed. The fitted models were conducted through an analysis of the variance (ANOVA). All the significant factors and results from the ANOVA are summarized in Tables 4-6. Statistical indicators *F*- and *t* values were then used to test significance of the analyzed factors. A significant level, α of 0.05 is used to test the entire null hypothesis. *p* value is the probability of obtaining a greater *F*- or *t* value due to a random error, provided that the null hypothesis is true in an *F*- or *t* test. *F*-test was adopted to verify the effectiveness of our developed empirical models by testing a null hypothesis that the model cannot provide a significant better fit than the mean of all experimental results; while *t*-test was adopted to determine the effectiveness of estimated parameters of each

model by testing a null hypothesis that the parameter is zero. The null hypothesis is rejected, if p value is smaller than 0.05 (i.e. $p < 0.05$). Factors that failed in a significant test ($p>0.05$) were eliminated, while the remaining factors were included in the models. In Table 5, the Total Sum of Squares (SST) is the sum of the squares (SS) of the differences between each experimental result and the mean of all the experimental results. The Sum of Squares of Error (SSE) is the sum of squared difference between each experimental result and the fitted line, corresponding to the unexplained variance in the regression model. The Sum of Squares of Model (SSM) is attributed to the difference between the SST and the SSE. F-value is defined as the ratio between the Mean Square Model (MSM) and the Mean Square Error (MSE). The R square, defined as the ratio of the SSM and SST was also used to assess effectiveness of the established model. In Tables 4 and 6, t-value was defined as the ratio of the estimated parameter to its standard error.

Comparisons between the predicted values and experimental results of additional experiments are shown in Table 7. Verifications of the established models were performed by testing the null hypothesis that there is no significant difference between the predicted values and experimental results in the t-test. This null hypothesis cannot be rejected if the p value is greater than 0.05 (i.e. $p > 0.05$).

Materials

Poly(L-lactide) (PLA) (Mw: ~20kDa), PLGA-mPEG (Mw: ~11kDa) was obtained from the Jinan Daigang biomaterials Co., Ltd. Dichloromethane (DCM), HCl and NH_3

Solution were purchased from the Merck & Co. Polyvinyl alcohol (Mw:~23kDa) and Tetraethylorthosilicate (TEOS) were acquired from Sigma-Aldrich. Vancomycin HCl (VC) was obtained from the Amresco.

Fabrication procedure of composite nanoparticles

Fabrication procedure of drug loaded silica xerogel/PLA composite nanoparticles is described in our previous work [12]. Briefly, TEOS, H_2O and HCl with a molar ratio of 1:20:0.0002 were mixed in a beaker under mild agitation, until a clear sol-gel solution was formed. The internal phase as the core material was prepared by dissolving 15 mg of vanconmycin HCl in a 1 ml of the as-prepared sol-gel solution. This internal phase was then ultrasonically homogenized through an ultrasonic cell crusher (SKL250-11N Ultrasonic cell crusher, Ningbo Haishu Sklon Electronic Instrument Co., Ltd) into a 10 ml polymer solution (shell material) to obtain a primary emulsion. 0.25 ml of 1% NH_3 solution was gradually added during preparation of the primary emulsion to initiate the gelation of the sol-gel drug solution. This polymer solution was prepared by dissolving 0.3g of PLA and 0.2g of PLGA-mPEG into 10 ml of DCM. The primary emulsion was then ultrasonically dispersed in 1.5% PVA aqueous solution to generate the secondary emulsion. The composite nanoparticles in the form of nano-suspension were obtained under 3 hours of mild agitation at room temperature. This nanoparticle suspension was centrifuged at 12000 rpm for 30 minutes by using a high-speed centrifuger (Model TG16-W, Hunan Xiangyi Centrifuge Instrument Co., Ltd). The supernatants were kept

for drug concentration analysis using UV/vis spectrophotometry (UV1102, Techcomp Ltd). The precipitated nanoparticles were washed three times with pure water before characterization.

Characterizations

Composite nanoparticle suspensions of 0.01 mg/ml were prepared prior to size measurement. The average size of composite nanoparticles was determined by a Zetasizer Nano ZS instrument (Malvern Instruments, Malvern, U.K.) at room temperature. The concentrations of VC in the supernatants were determined by measuring their absorbance by means of UV spectrophotometry at 280.5 nm. A standard curve, that was used to calibrate the relationship between the drug concentration and UV absorbance, was prepared using a drug concentration in a range of 0.6 ~ 0.032 mg/ml in 1.5% of PVA. It had a regression equation of y = 0.2347x+0.00942, with a correlation factor R of 0.996. The encapsulation efficiencies of the VC in the nanoparticles were determined by identifying the concentration of the non-encapsulated free drug in the supernatants after centrifugation of the nanoparticle suspension at 12000 rpm for 30 minutes. The EEs of the drug loaded nanoparticles were calculated through the following equation:

$$Encapsulation\ Efficiency\ (\%) = \frac{Total\ drug\ amount - Free\ drug\ amount}{Total\ drug\ amount} \times 100\%$$

RESULTS AND DISCUSSION

Empirical model of particle size

According to the results of *t* test presented in Table 4, all the four independent process variables, namely the sonication power of the second emulsion (*F1*), the ratio of W_2 phase and primary emulsion (*F2*), the volume of the second emulsion (*F3*) and the sonication time of the second emulsion (*F4*), have linear effects on the particle size. In addition to the linear effect, *F1* was found to possess a quadratic effect (*F1* x *F1*) on the dependence. Interactions were also observed between *F1* and *F2*, and between *F3* and *F4*. All these effects and interactions were significant since the *p* value of each influence was less than 0.05. The significances of these effects on the particle size are ranked in Fig.1. The effect of the sonication power (*F1*) on the particle size is the most significant and followed by the effect of *F2*, while *F3* has the least impact relative to the others.

An empirical model describing the relationship between all the significant effects and the response in terms of the particle size, *d* was determined and expressed by the following regression equation:

$$d = 537.93 - 3299.07 \cdot p_2 + 53.08 \cdot r + 3828 \cdot p_2^2 + 183.12 \cdot t_2 + 1.82 \cdot v_2 \cdot t_2 - 113.22 \cdot p_2 \cdot r + 1.84 \cdot v_2 \quad (8)$$

Effectiveness of the model has been verified, because the *p* value is much smaller that the significant level of 0.05 (Table 5). It can be observed from that the *R* square is 0.92

close to 1.00, indicating a goodness of fit for the model. For model verification of the equation (8), the relative mean standard deviation between the predicted values and experimental results were determined as in Table 7 and found to be acceptable with a value of 10.2%. There is no significant difference between the predicted values and experimental results in the *t*-test for the verification results ($p > 0.10$).

Empirical model of encapsulation efficiency

From Table 6, three independent process variables, namely the sonication power of the second emulsion (*F1*), the total volume of the second emulsion (*F3*) and the sonication time of the second emulsion (*F4*), were found to have significant linear effects on the encapsulation efficiency. Linear-linear interactions were discovered between *F1* and *F4*, and between *F1* and *F3*. No quadratic effect was observed from the empirical model of encapsulation efficiency. All the studied effects were significant, because all the insignificant effects were screened out during the statistical analysis. The most significant influence stemmed from the variable of the sonication power (*F1*), while the effect of interaction of *F1* x *F3* on the encapsulation efficiency was the weakest as shown in Fig.2.

The relationship between all the significant effects and the response - encapsulation efficiency was determined and can be expressed by the following regression equation

$$EE = 87.61 - 50.26 \cdot p_2 - 0.13 \cdot v_2 + 4.99 \cdot t_2 - 22.08 \cdot p_2 \cdot t_2 + 0.85 \cdot p_2 \cdot v_2 \quad (9)$$

From Table 6, the effectiveness of the established empirical model of encapsulation efficiency was confirmed, because of $p < 0.05$. The *R*-square value of the model from Table 5 is 0.902, indicating a goodness of fit between the predicted and experimental results. The results of verification for equation (9) are shown in Table 7, from which the relative mean standard deviation between the predicted values and the experimental results are found to be acceptable with a value of 5.08%. There is no significant difference between the predicted value and the experimental results in the *t*-test for the verification results ($p > 0.10$).

Effect of power of sonication

The sonication power of the second emulsion (*F1*) exhibited the most significant impact on both empirical equations among other effects. It can be observed from Figs. 3, 4 and 6 that increasing the power led to smaller particle size and lower EE, which was consistent with assumptions of equations (4) and (5) described in Section 2. This can be explained by the fact that increasing the sonication power output contributes to an augmented ultrasound cavitation effect. This effect led to an increase in the possibility of droplet break-up and delamination of the core-shell structure of the composite nanoparticles, which therefore resulted in more leakage of loaded drug during the second emulsion and hence lower EE and smaller particle size.

A quadratic effect of the sonication power on the particle size is observed from Fig.3. As the reduction of particle size was gradually mitigated, the minimum particle size was obtained, when the sonication power was increased to around 0.46 (representing 46% of the full power of 250W, namely 115W) at the lowest value of *r*. The sonication power of greater than 0.46 did not result in any significant change in the particle size. The impact of the sonication power was more significant at a higher value of *r*; while the threshold value of the sonication power output also increased from 0.46 to 0.54, which is discussed in detail in Section 4.4.

The effect of the sonication power on encapsulation efficiency exhibited a linear pattern. A significant reduction of the encapsulation efficiency along with increasing sonication power under the condition of long sonication time was found. This inverse relation was severely compromised with decreasing sonication time. A complete emulsion could not be formed and led to the formation of large particles during the limited sonication time as indicated in Fig.4, regardless of the high level of sonication power. When drug loaded core materials were trapped by a large amount of polymer in large particles, the possibility of drug leakage was reduced.

Effect of volume ratio of W_2 phase and primary emulsion

The volume ratio of W_2 phase and primary emulsion (r) was found to have significant impacts on particle size. It should be noted that *r*, which was assumed to have influence the EE according to the theoratical analysis in Section 2.2, was discovered to have no

significant relationship with the EE. Increasing the volume ratio, r leads to the formation of a larger particle size, as indicated in the equation (7). This effect was more significant at a lower level of the sonication power. Moreover, a higher value of volume ratio, r indicates that less energy is allocated to break up the dispersed phase (primary emulsion) during the second emulsion at fixed sonication powers. The allocated energy differences between the dispersed and continuous phased was ascribed to different values of volume ratio, r. However, these differences were not large enough to cause any further drug leakage and therefore their influences on the EE were limited.

Effect of total volume of the second emulsion

As illustrated in Figs.5 and 6, the total volume of the second emulsion (V_2) is significantly associated with both the size and EE of the prepared composite nanoparticles. Generally, growing volumes of the second emulsion can lead to increase of both the size and EE, which are consistent with the results of theoratical studies in Section 2.2. This can be attributed to the damping cavitation effects, when power density per unit volume is reduced at increasing V_2 with reference to equation (4). The changes of the particle size through altering the total volume were more significant under long sonication time. This resulted from the fact that a too short sonication time could lead to incomplete emulsification and thus generate a larger particle, even though the high sonication power, P_2 and low total volume, V_2 were applied.

With the same rationale, reduction of the sonication density caused by increasing V_2 due to low possibilities of particle breakage and high EEs are found as shown in Fig.6. This tendency was more conspicuous at higher sonication power level, which was associated with the different power density (P_v) gaps between the high and low sonication power outputs at different levels of sonication power. For instance, according to equation (4), the power density gap between the high (99 ml) and low (33 ml) volume of the second emulsion is 0.0040 for a sonciation power of 0.2. When a higher sonication power of 0.6 is applied, this gap significantly increases to 0.0121.

Effect of sonication time of the second emulsion

The sonication time of the second emulsion, t_2 is proportional to both the size and EE as shown in Figs.4 and 6. A relative complete emulsification and high possibility of particle breakage were realized using longer sonicaiton time, which was associated with the accumulated sonication energy of the emulsion. This engery, E_a for a range from 0 to t_2 is expressed as:

$$E_a = \int_0^{t_2} P_2 \, dt = P_2 t_2$$

It can be noted from this equation that a longer sonication time leads to higher energies and thus stronger cavitation effects, resulting in formation of smaller particles and lower EE as discussed previously in Section 2.2. This can be explained with the similar rationale as previsouly described in Section 3.5. The working engery gap of the high and low sonication time was larger at high sonication power, P_2 than that at low

sonication power.

Optimization strategy of particle size and encapsulation efficiency

A high encapsulation efficiency is always desirable, since it can prevent unnecessray wastage of drug. It was found that enhancement of the EE could be realized by reducing the sonication power, P_2, increasing the total volume of the sencond emulsion, V_2 or reducing the soncation time, t_2 as summarized in Table 8. The effectiveness of the aforesaid routes were ranked as $P_2 > t_2 > V_2$ according to the significance of difference process variables as shown in Fig.1.

The methods to reduce the size of the nanoparticles were found to include increase of the sonication power output, P_2 or the sonication time t_2; reduction of the volume ratio, r and the total volume of the sencond emulsion, V_2. The effectiveness of these routes was ranked as $P_2 > r > t_2 > V_2$ according to the significance of difference process variables as shown in Fig.2.

Unfortunately, when comparing the desirable strategies for acheiving both high encapsulation efficiency and small particle size as shown in Table 8, they are mutually exculsive. The relationship between the encapsulation efficiency and particle size is depicted in Fig.7. The solid line indicates the tendency of the measured data, while the dotted lines are the fitted lines with a 95% confidence level. From Fig.7, a significant reduction of the encapsulation efficiency for fabricating the particle with a size of

smaller than 500 nm can be observed, confirming that the particle size is proportional to the encapsulation efficiency as revealed from the theoretical studies in Section 2.2.

This mutually exclusive effects for desirablility of the particle size and encapsulation efficiency indicated a principle that negative impacts on EE needed to be minimized, when desgining a combination of process variables to produce the particle size toward a desirable value. Based on this principle, in order to minimize the negative impact on the encapsulation efficiency for the case of samller particle fabrication, an optimization strategy is proposed that adjustment of the particle size toward the target value should start from changing the process variables that have the least negative impact on the EE and maintain the other process variables at the favorable position of EE. The effects and significances of the impacts of different process variables on the responses are listed with a ranking from left to right in Table 8. The optimization strategy is illustrated in Fig.8. Starting from a combination of process vairables (P_2 = 0.2, r = 8, t_2 = 0.5, V_2 = 99) that gave the largest particle size (913.7 nm) and the optimal encapsulation efficiency (80.48%), the route to explore an optimal combination of process variables for the target particle size was to reduce the particle size from the largest value (913.7 nm) by adjusting process variables in the order of r, V_2, t_2, P_2 until reaching the target size or a minimal value (size: 89.7nm, EE: 43.46%) at a combination of P_2 = 0.6, r = 2, t_2 = 3, V_2 = 33 as shown in Fig.8.

In most investigations, adjustment of the second sonication time, t_2 is widely adopted routes for tailoring the particle size, which, however, is not an optimal strategy. For

isntance, by setting the combination of other process variablesas $P_2 = 0.6$, $r = 8$,$V_2 = 33$, a minimum size of 211 nm and encapsulation efficiency of 27% can by obtained by adjusting the second sonication time, t_2 with a combination of the process variables as ($P_2 = 0.6$, $r = 8$, $t_2 = 3$, $V_2 = 33$). Following our optimization strategy, a much better encapsulation efficiency of 63% was obtained for a size of around 211 nm by using an combination of optimal process variables as ($P_2 = 0.29$, $r = 2$, $t_2 = 3$, $V_2 = 33$). The improvement of degreee of encapsulation efficiency was found to range from several percentages to a tens of percentages for different target particle sizes. All of these illustrations have proved the effectiveness and benefits of applying our developed optimization strategy.

CONCLUSIONS

The optimization strategy to explore optimal combinations of the screened significant process variables of our recently developed gelation emulsion method, including sonication power of the second emulsion (P_2), volume ratio (r), volume of the second emulsion (V_2) and sonication time of the second emulsion (t_2), for producing a target particle size with an optimal encapsulation efficiency, has been successfully established. To develop the optimization strategy, linear and quadratic effects and the interactions of the significant process variables on the size and encapsulation efficiency (EE) of the drug loaded silica xerogel/PLA composite nanoparticles have been analyzed through a 4-factor central composite face-centered experimental design and analysis of the

variance. The strategy for producing the target particle size with an optimal encapsulation efficiency was achieved by adjusting the process variables in the order of r, V_2, t_2 and P_2.

With the developed optimization strategy, the encapsulation efficiency of the prepared nanoparticles was significantly enhanced as compared with that obtained by the widely adopted route of mainly adjusting the second sonication time. For instance, the encapsulation efficiency of the nanoparticles has been improved from 27% to 63% for a size of around 211 nm. By considering the interactive effects among all the significant process variables in this study, the feasible particle size range has substantially widened to 90 - 914 nm as compared with the range of 192 -569 nm obtained from our previous work without the optimization strategy. This broaden operation window allow the fabrication of nanoparticles of various size requirements for wider application. This useful optimization strategy can not only be applied to the gelation-emulsion method but also to other double emulsion processes for minimizing the negative impacts on the EE, especially for the case of fabricating small nanoparticles required for drug delivery application.

ACKNOWLEDGMENTS

The authors would like to thank the support from the Research Committee of The Hong Kong Polytechnic University (Project No.: RTE9).

REFERENCES

1 F. Danhier, E. Ansorena, J. M. Silva, R. Coco, A. Le Breton and V. Preat, *Journal of controlled release : official journal of the Controlled Release Society* **161:**505-522 (2012).

2 A. Kumari, S. K. Yadav and S. C. Yadav, *Colloids and surfaces B, Biointerfaces* **75:**1-18 (2010).

3 D. Brambilla, P. Luciani and J. C. Leroux, *Journal of controlled release : official journal of the Controlled Release Society* **190:**9-14 (2014).

4 V. Lassalle and M. L. Ferreira, *Macromolecular bioscience* **7:**767-783 (2007).

5 C. E. Mora-Huertas, H. Fessi and A. Elaissari, *International journal of pharmaceutics* **385:**113-142 (2010).

6 M. Iqbal, N. Zafar, H. Fessi and A. Elaissari, *International journal of pharmaceutics* **496:**173-190 (2015).

7 J. W. Hickey, J. L. Santos, J. M. Williford and H. Q. Mao, *Journal of controlled release : official journal of the Controlled Release Society* **219:**536-547 (2015).

8 M. Azizi, F. Farahmandghavi, M. Joghataei, M. Zandi, M. Imani, M. Bakhtiary, F. A. Dorkoosh and F. Ghazizadeh, *Journal of Polymer Research* **20:**(2013).

9 M. Ayoub, N. Ahmed, N. Kalaji, C. Charcosset, A. Magdy, H. Fessi and A. Elaissari, *Journal of Biomedical Nanotechnology* **7:**255-262 (2011).

10 S. Prasad, V. Cody, J. K. Saucier-Sawyer, T. R. Fadel, R. L. Edelson, M. A. Birchall and D. J. Hanlon, *Pharmaceutical research* **29:**2565-2577 (2012).

11 A. Schuch, L. G. Leal and H. P. Schuchmann, *Colloids and Surfaces A: Physicochemical and Engineering Aspects* (2013).

12 W. F. Huang, G. C. P. Tsui, C. Y. Tang and M. Yang, *Composites Part B: Engineering* **95:**272-281 (2016).

13 S. Mao, J. Xu, C. Cai, O. Germershaus, A. Schaper and T. Kissel, *International journal of pharmaceutics* **334:**137-148 (2007).

14 Z. Wang, *Journal of Applied Polymer Science* **115:**2599-2608 (2010).

15 T. Feczkó, J. Tóth, G. Dósa and J. Gyenis, *Chemical Engineering and Processing: Process Intensification* **50:**846-853 (2011).

16 T. Feczkó, J. Tóth, G. Dósa and J. Gyenis, *Chemical Engineering and Processing: Process Intensification* **50:**757-765 (2011).

17 K. Park, *Journal of controlled release : official journal of the Controlled Release Society* **190:**3-8 (2014).

18 A. K. Mitra, V. Agrahari, A. Mandal, K. Cholkar, C. Natarajan, S. Shah, M. Joseph, H. M. Trinh, R. Vaishya, X. Yang, Y. Hao, V. Khurana and D. Pal, *Journal of controlled release : official journal of the Controlled Release Society* **219:**248-268 (2015).

19 D. Wen, M. Danquah, A. K. Chaudhary and R. I. Mahato, *Journal of controlled release : official journal of the Controlled Release Society* **219:**237-247 (2015).

20 Y. Chen, S. Zhou and Q. Li, *Acta biomaterialia* **7:**1140-1149 (2011).

21 S. Fredenberg, M. Wahlgren, M. Reslow and A. Axelsson, *International journal of pharmaceutics* **415:**34-52 (2011).

22 M. C. Costache, H. Qu, P. Ducheyne and D. I. Devore, *Biomaterials* **31:**6336-6343 (2010).

23 S. Radin, T. Chen and P. Ducheyne, *Biomaterials* **30:**850-858 (2009).
24 L. P. Singh, S. K. Bhattacharyya, R. Kumar, G. Mishra, U. Sharma, G. Singh and S. Ahalawat, *Advances in colloid and interface science* **214C:**17-37 (2014).
25 R. Ciriminna, A. Fidalgo, V. Pandarus, F. Beland, L. M. Ilharco and M. Pagliaro, *Chem Rev* **113:**6592-6620 (2013).
26 J. Stergar and U. Maver, *Journal of Sol-Gel Science and Technology* **77:**738-752 (2016).
27 Z. Ulker and C. Erkey, *Journal of controlled release : official journal of the Controlled Release Society* **177:**51-63 (2014).
28 J. Kurczewska, P. Sawicka, M. Ratajczak, M. Gajecka and G. Schroeder, *International journal of pharmaceutics* **486:**226-231 (2015).
29 A. Soleimani Dorcheh and M. H. Abbasi, *Journal of Materials Processing Technology* **199:**10-26 (2008).
30 M. Alnaief, S. Antonyuk, C. M. Hentzschel, C. S. Leopold, S. Heinrich and I. Smirnova, *Microporous and Mesoporous Materials* **160:**167-173 (2012).
31 M. C. Costache, A. D. Vaughan, H. Qu, P. Ducheyne and D. I. Devore, *Acta biomaterialia* **9:**6544-6552 (2013).
32 L. Al Haushey, M. A. Bolzinger, C. Bordes, J. Y. Gauvrit and S. Briancon, *International journal of pharmaceutics* **344:**16-25 (2007).
33 S. Kim, J. C. Kim, D. Sul, S. W. Hwang, S. H. Lee, Y. H. Kim and G. Tae, *Journal of Nanoscience and Nanotechnology* **11:**4586-4591 (2011).
34 B. Tal-Figiel, *Chem Eng Res Des* **85:**730-734 (2007).
35 T. Tadros, R. Izquierdo, J. Esquena and C. Solans, *Advances in colloid and interface science* **108:**303-318 (2004).
36 A. Gedanken, *Ultrason Sonochem* **11:**47-55 (2004).
37 C. Leonelli and T. J. Mason, *Chemical Engineering and Processing: Process Intensification* **49:**885-900 (2010).
38 P. Walstra, *Chemical Engineering Science* **48:**333-349 (1993).
39 T. S. H. Leong, T. J. Wooster, S. E. Kentish and M. Ashokkumar, *Ultrasonics Sonochemistry* **16:**721-727 (2009).

List of Tables

List of Figures

Figure 7 Relationship between average particle size and encapsulation efficiency. The solid curve represents the relationship; while the gap between two dashed curves indicate a 95% confident interval for the solid curve.

Figure 8 Strategy to determine an optimal combination of process variables (Remark.↓: decrease; ↑: increase)

Table 1 Theoretical trend estimations of different process variables

Process variables	P_2	r	V_2	t_2
Encapsulation efficiency	+	-	-	+
Particle size	+	-	-	+

* "+" represents a direct proposition; "-" represents an inverse ratio

Table 2 Selected process variables and corresponding study range

Symbol	Variable	Intervals
P_2	Sonication power of the second emulsion*	0.2-0.6
r	Volume ratio of W_2 phase and primary emulsion	2-8 v/v
V_2	Total volume of the second emulsion**	33-99 ml
t_2	Sonication time of the second emulsion	0.5-3.0 min

* Full power output of ultrasonic device was 250W. 0.2 sonication power output indicated 20% of full power, namely 50W.

Table 3 A series of 27 experiments designed by CCF method and corresponding results

Run No.	F1	F2	F3	F4	Response	
	P_2	r	t_2 (mins)	V_2 (ml)	EE%	Mean Size (nm)
1	0.2	8	0.5	99	85.3	872.0
2	0.6	2	3	33	16.5	247.6
3	0.6	8	3	99	45	412.0
4	0.2	8	3	99	78.3	944.0
5	0.4	5	1.75	66	65.5	354.0
6	0.6	8	0.5	33	80.5	725.8
7	0.6	2	3	99	76.4	1044.0
8	0.2	2	0.5	33	64.6	535.2
9	0.6	8	0.5	99	89.4	508.0
10	0.2	8	0.5	66	71.9	399.0
11	0.2	2	3	33	72.2	525.3
12	0.6	2	0.5	33	28.8	288.9
13	0.4	5	1.75	99	70.2	610.9
14	0.2	2	0.5	66	77.4	622.6
15	0.6	8	3	66	66.3	323.8
16	0.2	8	3	99	73.6	269.9
17	0.2	2	3	33	78.7	437.8
18	0.6	2	0.5	33	69.7	398.5
19	0.4	2	1.75	99	66.2	336.5
20	0.4	5	1.75	33	69.1	476.7
21	0.4	8	1.75	66	67.2	412.7
22	0.4	5	1.75	66	61.1	312.6
23	0.6	5	1.75	99	58.4	362.8
24	0.2	5	1.75	66	80	745.5
25	0.4	5	0.5	33	78.3	500.0
26	0.4	5	3	66	60	304.0
27	0.4	5	1.75	66	70.5	397.0

Table 4

t-test for the significance of parameter estimates for particle size

Term	Estimate	*t* value	*p* value
Intercept	393.0000	17.19	<0.0001
F1	-160.5500	-9.9291	<0.0001
F2	91.3333	5.6484	<0.0001
F3	44.0944	2.7270	0.0134
F4	-78.7778	-4.8719	0.0001
F1 x *F2*	-67.9250	-3.9605	0.0008
F3 x *F4*	75.0625	4.3767	0.0003
F1 x *F1*	153.1167	5.4671	<0.0001

Table 5

ANOVA test for the significance of models

Particle Size (*R* Square:0.9226)				Encapsulation Efficiency (*R* Square:0.9017)			
Source	DF	Sum of Squares	*F* value	Source	DF	Sum of Squares	*F* value
Model	7	1065469.3	32.3421	Model	5	5915.8124	38.5398
Error	19	89418.6	*p* value	Error	21	644.6950	*p* value
Total	26	1154888.0	< 0.0001	Total	26	6560.5074	< 0.0001

Table 6

t-test for the significance of parameter estimates for encapsulation efficiency

Term	Estimate	*t* value	*p* value
Intercept	67.4482	63.25	<0.0001
F1	-10.0389	-7.6870	<0.0001
F4	-9.8000	-7.5040	<0.0001
F3	6.8278	5.2282	<0.0001
F1 x *F4*	-8.0188	-5.7889	<0.0001
F1 x *F3*	5.6188	4.0563	0.0006

Table 7

Predicted and observed values of mean particle size and encapsulation efficiency for model verification

Process Variable					Mean size(nm)		Encapsulation Efficiency (%)	
Run	*F1*	*F2*	*F3*	*F4*	Predicted Value	Observed Value	Predicted Value	Observed Value
1	0.25	8	99	1.5	786.66	720.00	78.34	78.53
2	0.25	8	99	0.5	789.62	746.60	81.38	80.24
3	0.35	8	99	1.5	595.86	551.90	76.94	74.86
4	0.35	8	99	0.5	598.83	573.00	83.17	80.33
5	0.6	2	33	1.5	348.83	286.70	48.53	49.34
6	0.45	2	33	1.5	274.76	304.50	59.07	53.22
7	0.35	2	33	0.5	444.14	386.10	72.30	76.08
8	0.35	2	33	1.5	321.06	335.80	66.09	71.80
9	0.35	2	33	2.5	197.99	251.60	59.80	64.03
10	0.4	5	66	1.8	389.85	407.00	67.05	70.74

Table 8

Confirmed trend of different process variables

Response	Desirability	Process variable*			
		P_2	r	t_2	V_2
Encapsulation efficiency	↑	↓	/	↓	↑
Particle size	↓	↑	↓	↑	↓

*Process variables are listed according to their significance to the response in an order from left to right. (e.g. The significance for encapsulation efficiency, $P_2 > t_2 > V_2$; for particle size: $P_2 > r > t_2 > V_2$.)

Table 9

List of Symbols

Symbols	
P_2	Sonication power of the second emulsion
r	Volume ratio of W_2 phase and primary emulsion
V_2	Volume ratio of W_2 phase and primary emulsion
t_2	Sonication time of the second emulsion
σ	Interfacial surface tension
p	Laplace pressure
R	Radius of spherical droplets
B,C	Constant
P_v	Sonication power density, W/ml
ρ	Density of continuous phase
d_{max}	Maximum droplet diameter
d_{av}	Average droplet diameter
P_t	Sonication power, W
V	Volume of emulsion ($V_d + V_c$)
V_d	Volume of dispersed phase
V_c	Volume of continuous phase
E	Energy output of sonication over time
E_a	Accumulated Energy of the emulsion over time

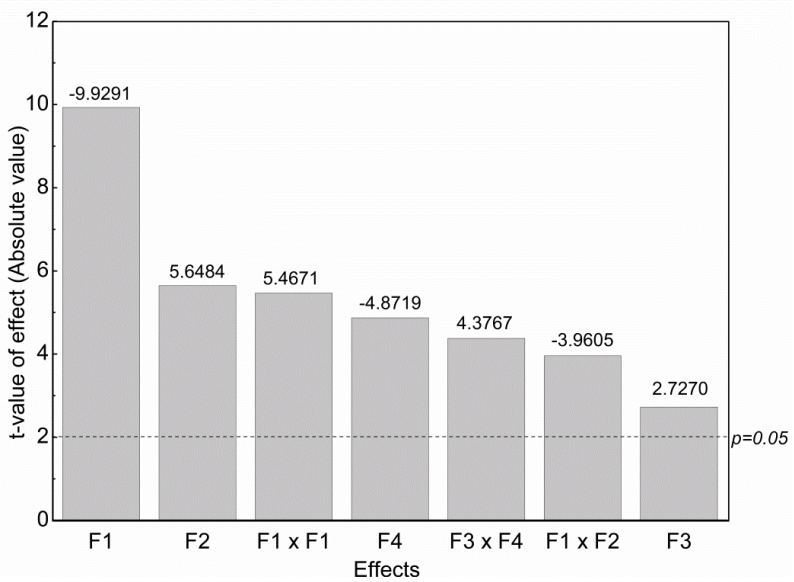

FIG.1. Pareto chart of significant effects on particle size

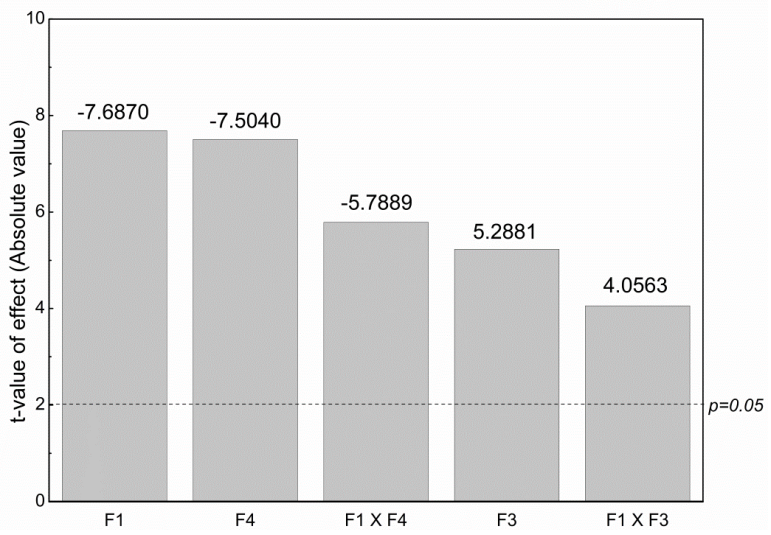

FIG.2. Pareto charts of significant effects on EE

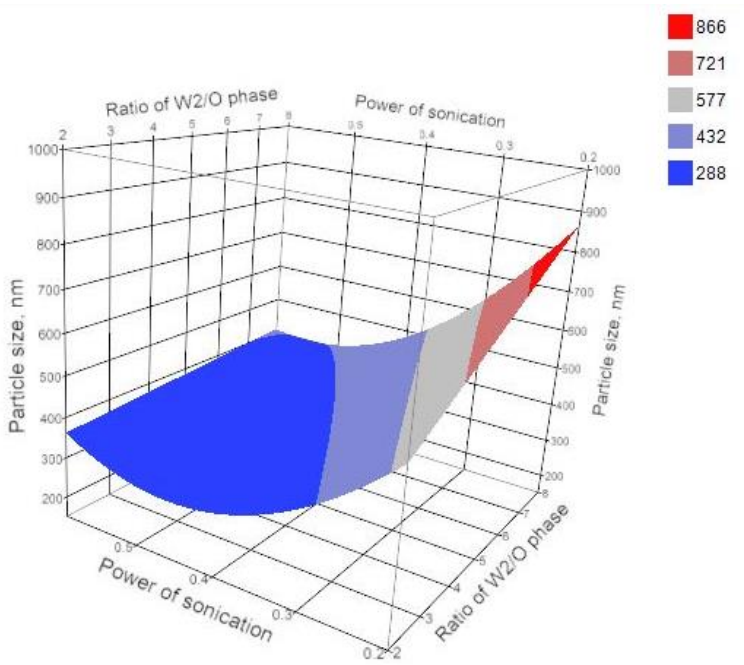

FIG.3. Effect of soncation power and ratio of W_2 phase and primary emulsion (t_2= 1.75mins; v_2=66 ml). Different colors on the surface correspond to different particle sizes as shown in the legend

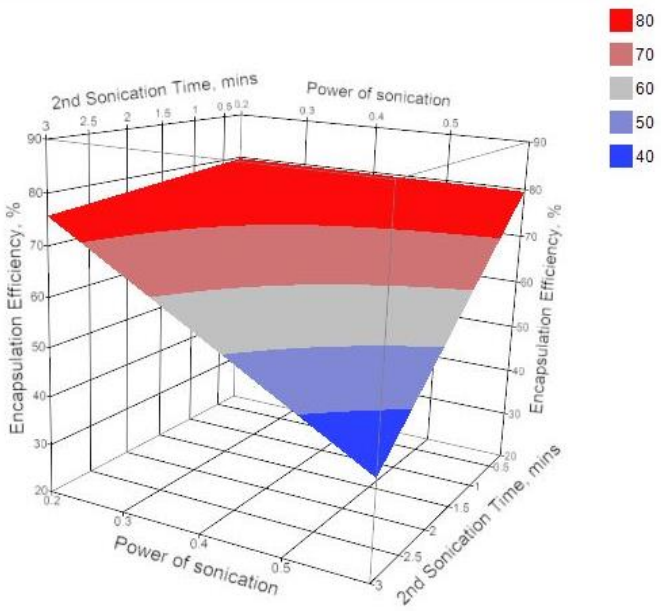

FIG.4. Effect of sonication power and sonication time of the second emulsion (v_2= 66 ml; r = 5). Different colors on the surface correspond to various levels of encapsulation efficiency as shown in the legend.

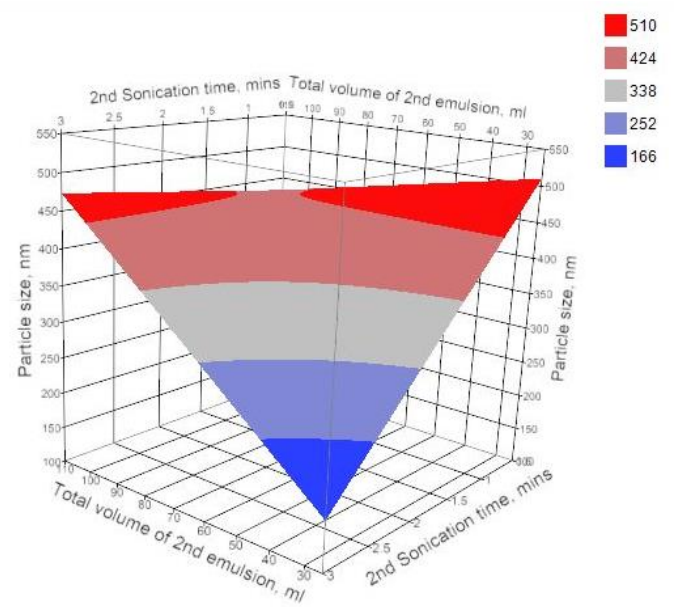

FIG.5. Effect of total volume of the second emulsion and sonication time of the second emulsion (P_2= 0.4; r = 5). Different colors on the surface correspond to various levels of encapsulation efficiency as shown in the legend.

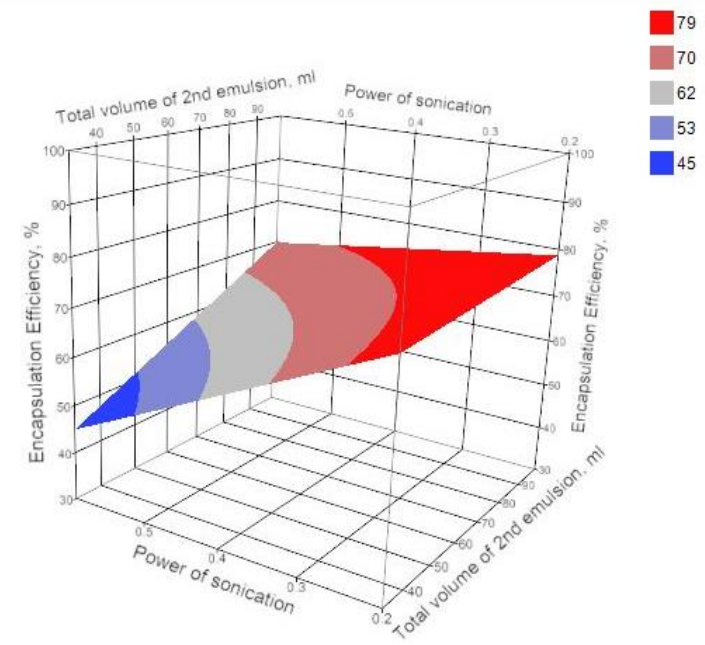

FIG.6. Effect of sonication power and total volume of the second emulsion (V_2= 66 ml; r = 5). Different colors on the surface correspond to various levels of encapsulation efficiency as shown in the legend.

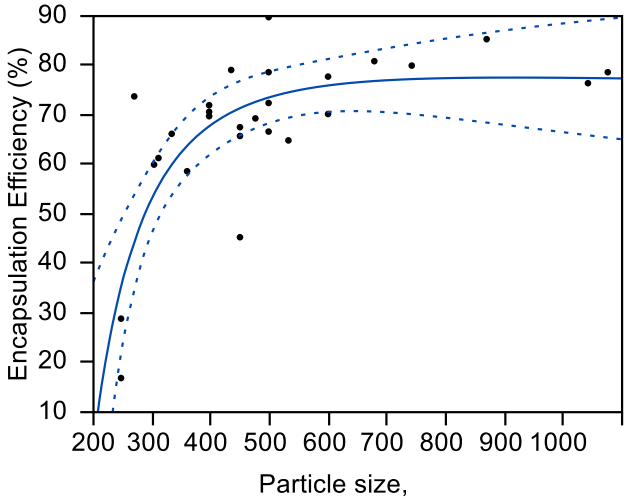

FIG.7. Relationship between average particle size and encapsulation efficiency

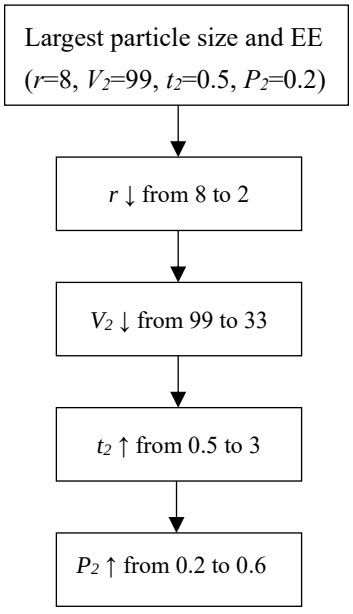

FIG.8. Strategy to determine an optimal combination of process variables
(Remark.↓: decrease; ↑: increase)